

GENERATION OF ROOF TOPOLOGIES USING PLANE FITTING WITH RANSAC

J. Engels, H. Arefi and M. Hahn

Stuttgart University of Applied Sciences, Germany
{johannes.engels, hossein.arefi, michael.hahn}@hft-stuttgart.de

Commission III, WG III/3

KEY WORDS: LIDAR, RANSAC, building reconstruction, roof topology, city models, rule-based approach

ABSTRACT:

For the acquisition of Digital Surface Models (DSM), LIDAR has proven a reliable and accurate observation technique. In contrast to the generation of a Digital Terrain Model, which can be derived from the corresponding DSM by morphological filtering, the extraction of building models from the DSM requires more sophisticated modelling techniques. Here we follow a data-driven approach. The high density of recorded airborne LIDAR data inspires to develop concepts which are relying on the bulk of data. Accordingly, we have decided to reconstruct building models from LIDAR data by fitting surface planes with the well-known RANSAC technique. After the mere plane fitting, plane regions have to be formed and adjacent plane regions are intersected. A possible separation of roof faces by vertical walls is taken into account. By exploiting the established neighbourhood relations of all plane regions and the computed intersection lines the 3D coordinates of corner points of the building can be estimated. A global adjustment is performed in which corrections to the plane parameters are provided in order to conserve the planarity of the polyhedral surfaces. Our main focus in this paper, however, is the creation and reorganization of the roof topology. Insignificant structures in the building model have to be eliminated; this corresponds to unifications or splitting of corner points. It is crucial to preserve consistency within the reorganization process. In particular, in the horizontal projection of the roof, the edges are allowed to intersect only in the corner points. The polygons confining the planar roof surfaces have to be closed and consistently oriented. The paper proposes rules for the reorganization of the topology and illustrates our overall approach for building reconstruction with an example.

1. INTRODUCTION

Intensive research has been carried out during the last decade to develop algorithms for the collection of 3D city models. At first aerial and space images have been used as primary sources for the 3D measurements, later on the interest of the research community was attracted by LIDAR data. An excellent overview is given by (Baltsavias et al. 2001) and (Vosselman and Brenner 2005). Today, a number of semiautomatic and automatic approaches are proposed which are using airborne stereo imagery or airborne LIDAR data. Furthermore, the integration of both, LIDAR data and aerial images, is stressed in order to improve the algorithmic developments (Schenk and Csatho 2002).

Here we follow a data-driven, generic approach to reconstruct buildings from LIDAR data. The fundamental steps are to segment the data into planes and to combine these planes to a polyhedral model (Vosselman 1999, Rottensteiner 2003, Alharty and Bethel 2004). The advantage of those generic approaches is their high adaptability to complex shapes and to great details of buildings, in particular to roof structures. In a recent work (Tarsha-Kurdi et al. 2007) compared a Hough transform and a RANSAC based technique for automated detection of building roof planes and concluded that the RANSAC algorithm was more reliable in detecting the roof planes.

It seems to be more promising to fit 2D or 3D parametric models like surface planes or 3D primitives to the LIDAR DSM than to extract edges or corners from the LIDAR point cloud: With the former technique we are relying on the bulk of data, not on a small subset of points featuring extreme curvature or more general discontinuity measures. The interpolation of the original LIDAR data on a regular grid is frequently blurring the discontinuities in the LIDAR DSM. Accordingly, we have decided to reconstruct building models from LIDAR DSMs by fitting surface planes with the well-known RANSAC technique. Whereas

RANSAC was originally developed for robust estimation of the model parameters of one single model, it can be likewise applied for the fitting of an a priori unknown number of models to a dataset. The procedure simply has to be performed repeatedly. Points which have been found to be compatible with a particular model are marked. Careful tuning of the thresholds is indispensable.

After the mere plane fitting, plane regions have to be formed from the subsets of points which are compatible with the individual planes. This can be achieved by morphological filtering, in particular majority filtering. By connectivity analysis we obtain the region boundaries in the horizontal plane and the corresponding adjacency matrix. With the term "*boundary piece*" we denote in the following a continuous (uninterrupted) border between two adjacent regions. We shall call the ends of the boundary pieces *nodes*. Obviously from any node at least three boundary pieces emanate. A special case of boundary pieces are closed ones which do not feature nodes.

We assume that the building outlines are given, possibly as sequences of connected points. So far the boundaries of the regions are irregular, they are to be approximated by linear segments. We intersect the planes of adjacent regions. As roof faces which are neighbored in the horizontal plane may actually be separated by vertical walls, we have to check for any intersection line if its horizontal projection is compatible with the corresponding region boundary in the horizontal plane. Otherwise an approximation of the region boundaries in the horizontal plane can suitably be achieved by a 2D-RANSAC fit. We call the first type of edges in the horizontal plane *intersection edges* (I-edges), the second type of edges *jump edges* or *discontinuity edges* (D-edges).

As more than two accepted edges which should end in a common corner in general do not intersect each other in the same point, the positions of the building corners have to be computed

by an adjustment. Here a local adjustment for the corner coordinates is insufficient, as the planarity of the polyhedral surfaces is to be conserved. Therefore, a global adjustment is performed in which the plane and D-edge parameters are considered as observations and the corner coordinates as unknowns. As conditions we impose that the building edges must intersect each other in the corner points. Since the conditioned adjustment with unknowns may lead to ill-conditioned normal equations, we use the common Gauss-Markov model and take the conditions as pseudo-observations into account.

The main focus in the paper is laid on the creation and reorganization of the roof topology (Section 2). The mathematical formulation of the global adjustment is presented in Section 3 and first results of the implemented algorithms are discussed and visualised in Section 4.

2. AN ALGORITHM FOR THE CREATION AND REORGANIZATION OF THE ROOF TOPOLOGY

2-1 General Considerations

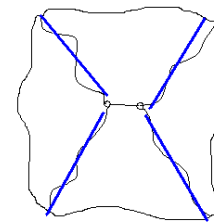
Whereas the term topology features different aspects in mathematics, we shall use it here in the sense of “adjacency relations”. Since we restrict ourselves to a $2\frac{1}{2}$ -D consideration, i.e. since we assume that the *outward* normal of each plane has a z-component bigger or equal to zero, the establishment of the topology can be performed essentially in the horizontal plane. Admittedly, vertical walls require an additional consideration as the directions of their outward normals are indeterminable from a 2D view.

As we have already identified regions, boundary pieces and nodes, a *preliminary topology* is already established, regardless of the edges which have been fitted. However, this preliminary topology in general cannot be accepted as the final one. On the one hand it might be inconsistent with the corresponding *geometrical* situation as defined by the edges, in particular if intersections between two subsequent edges are far from their provisional endpoints. On the other hand, it might be unnecessarily complicated, e.g. if very short boundary pieces without any fitting edges (“empty boundary pieces”) exist, which prevent the preceding and the succeeding edge to intersect as they “naturally” should. In general, we consider the parameters of the so far determined geometric elements, in particular the plane parameters, as much more reliable than the preliminary topology. Whereas the plane parameters are supported from a bulk of fitting points, the preliminary topology depends frequently on the affiliation of few pixels in the vicinity of the nodes and therefore may have been affected by blurring effects in the data and even more by the morphological filter process.

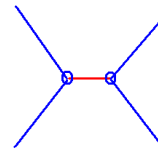
That means, we have to reorganize the topology, taking into account the geometrical situation as given by the edges which have been accepted so far. In particular, we have to decide which regions are adjacent to each other, which edges meet in a corner, which edges should be eliminated or newly introduced, see figure 1 as an example. Figure 1(a) illustrates the accepted elements, the preliminary topology is induced by the irregular boundary pieces only. Figures 1(b) – 1(e) show possible alternative topologies.

Evidently, we may use the preliminary topology as a first guess and improve it stepwise until our requirements are fulfilled. As *geometric* criteria for establishing the topology we use the following:

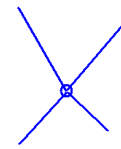
1. The so-far accepted elements planar regions and edges must be retained.



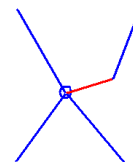
(a) Preliminary topology and fitted edges



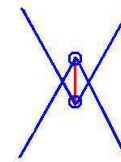
(b) Edges according to preliminary topology (red edge inserted)



(c) Reorganized topology I



(d) Same as figure 1c, additional edge inserted



(e) Reorganized topology II (non-admissible)

Figure 1: Reorganization of topology: Problem and possible solutions

2. New planar regions must not be introduced.
3. The parameters of the so-far accepted elements should be changed as sparsely as possible.
4. There should be as few corners as possible.
5. Short edges (also vertical ones) should be avoided.
6. Acute angles should be avoided.

The first two criteria in contrast to the others are “must”-requirements, for which we shall permit only rare exceptions. It is obvious that the stated requirements partly contradict. For the situation of figure 1, e.g., we have to choose between a relatively short new edge and a relative small distortion of the accepted edges. Generally, the more additional edges are introduced, the weaker are the constraints which may enforce changes of the so-far computed parameters.

2-2 2D Model Consistency

We deal with 2D model consistency on three levels; the first two are related to *topological*, the last one to *geometrical* concepts.

2-2.1 Level 1: We may represent the roof topology by an undirected *graph*, which is defined by the nodes and the existing connections between these nodes. The connections can be identified with the boundary pieces, of course. For this level, we claim the following consistency conditions:

- 1a) Every node must have at least two neighbours, i.e. should be connected to at least with two other nodes, unless it is connected to itself.

1b) Each connection must appear at least in one closed path, i.e. in a sequence of connected nodes where the start node is the same as the end node and no connection is used twice.

1c) The graph must be planar.

Conditions 1a), 1b) ensure that the topology features no one-dimensional parts; condition 1b) is excluding cases like figure 2(a). Condition 1c) means that the graph *can* be visualized in a planar representation without crossing connections. Figure 2(b) shows an example where condition 1c) is violated. Figure 2(c) on the contrary is planar; on the current level of definition it is equivalent to figure 2(d).

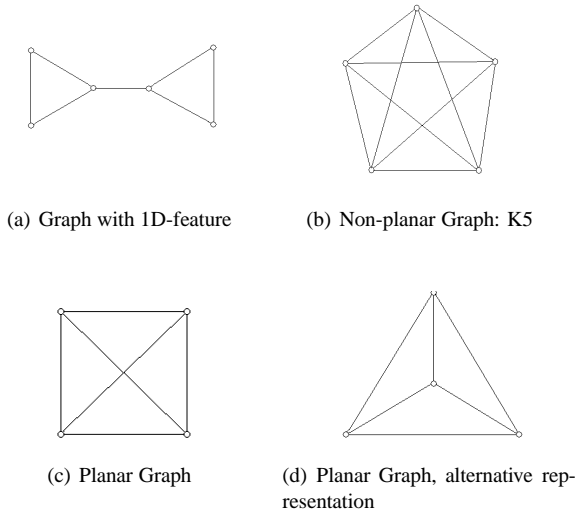


Figure 2: Examples for 2D-topologies

2-2.2 Level 2: As the main result of the RANSAC algorithm are planar segments, it will be helpful to introduce an additional topological element “*face*” which can be identified with the 2D region. Lateron, we shall assign 2D-coordinates to the nodes and thereby establish a distinct planar representation of the graph; for this representation the faces should form a complete and disjoint (non-overlapping) segmentation of the plane. On the current (still topological) level, however, we define *faces* without referring to geometric concepts. First we introduce a *cyclic ordering* of the connections which are emanating from a node. (On the geometric level we shall order the connections according to the azimuths of the emanating edges in a clockwise sense. With this interpretation of the ordering, figures 2(c) and 2(d) become distinguishable.) Once an ordered sequence of connections is established for each node, we are able to define *loops* by the following rule:

Select a node and a connection starting from this node. Then repeat the following procedure:

Search the corresponding end node of the current connection and identify the connection in the connection list of this end node. Select the next connection in this list ...

until the current node equals the starting node and the current connection equals the starting connection.

The sequence of nodes obtained in such a way we call a *loop*. Note the fundamental difference between a closed path as appearing in condition 1b) and a loop: In the former we are free in each step to choose the next connection, in the latter not. With the given definition of a loop, we have also established an *orientation*, as the reversed sequence of the nodes of a loop in general

does not correspond to a loop any more. We now claim a further condition for topological consistency:

2*) In any loop no connection must appear twice.

With this condition we may exclude cases of crossing connections as in figure 2(c).

With the concept of loops we are now ready to define: A *face* is an object which is delimited by exactly one outer loop and arbitrarily many (possibly zero) inner loops. What is an “inner” and what is an “outer” loop is up to our declaration, so far. We admit exactly one exceptional face which features only inner loops. This face we call *complementary face*, it corresponds to the region outside the building, but does not include inner court yards. With the definition of faces given, we require the following consistency conditions, which are partly redundant with condition 2*):

2a) Each connection must appear in the boundary (i.e. in the delimiting loops) of exactly two faces.

2b) At least for one of the two faces the connection must be part of an outer loop.

2c) The connection must have opposite orientation within the respective loops of the adjacent faces.

An overall check for the consistency of the topology is given by the well-known Euler-Poincaré theorem. This theorem can be formulated in different ways. Very convenient is the formulation given by (C. Séquin):

$$I - N_0 + N_1 - N_2 + N_3 - \dots - N_D = R_1 - R_2 + R_3 - \dots - R_D. \quad (2-1)$$

Here I denotes the number of individual, non-connected assemblies, N_0 the number of nodes, N_1 the number of connections, N_2 the number of faces etc. R_1 is the number of closed ring “connections”, R_2 the number of annular, ring-shaped faces, R_3 the number of solid-body handles. As the dimension D in our case is 2, we are faced with objects up to index 2 only. The equation represents a necessary condition for consistency.

2-2.3 Level 3: Finally we take into account the *geometrical relationships*. On this level, the nodes and corners are equipped with 2D coordinates. The connections between the nodes are assumed to be combinations of linear segments in \mathbb{R}^2 . It is to be emphasized that the latter assumption is not yet fulfilled by the “preliminary” elements!

We add the following consistency conditions:

3a) The ordering of the connections emanating from a node must feature ascending azimuths of the corresponding edges.

3b) Inner loops of a face have to be situated completely inside the outer loop of the face.

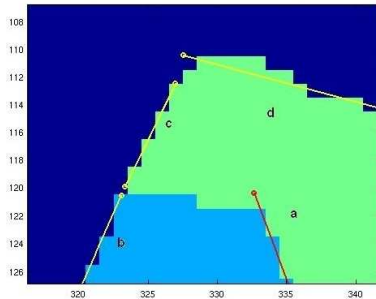
3c) Inner loops of a face must not overlap. The edges of the inner loops of a face must not intersect or touch each other except in the registered nodes.

3d) Edges of a loop must not intersect or touch each other, except neighbored edges in the registered nodes or corner points.

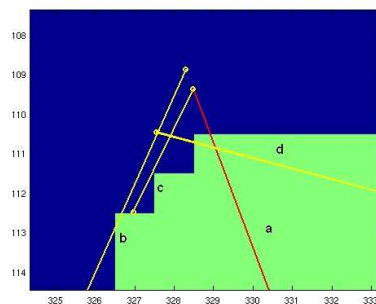
The preliminary topology fulfills the requirements 1a) - 1c) and 2a) - 2c) automatically. Inconsistencies on the former two levels may occur by redundancies in the data structure, e.g., if the list of connections departing from a node is incompatible with the

corresponding loops defining the faces. This can be avoided by correct implementation.

The conditions of the current level might be violated, for instance, if two accepted neighbored edges of a loop are linked by intersecting them: The edges might be elongated and intersect other edges of the loop polygon. Figure 3 shows an example: Edge a is



(a) Preliminary topology and fitted edges



(b) Reversal of edge c due to intersection with edge a

Figure 3: Computation of approximate node coordinates, for explanations see text

an accepted I-edge, edges b, c, d are accepted D-edges. The region in dark blue is the exterior of the building. Edges c, d belong to the same boundary piece, whereas the questionable node features the edges a, b, c. Obviously the intersection point between a and c is situated even beyond the “far end” (far from the node) of c. And since the footpoint of this intersection is accepted as the new endpoint of edge c at the side of the node, the direction of c will be reversed, as is shown in figure 3(b)! Edge d is not incident to the node, but anyway intersected now by the edges a and b. To avoid such reversals of edges, we permit an exception from the rule, that a fitted (accepted) edge must not be eliminated any more.

Conditions 3b, c can be verified with point-in-polygon algorithms; condition 3d can be verified by intersecting the non-neighbored edges of a loop and checking if the intersection point is situated between the endpoints of the two edges, respectively. Condition 3a) is redundant, but can be used as a criterion for the unification of nodes, see section 2–5.

2–3 Topological operations

Which operations are to our disposal in order to change the preliminary topology? Just inserting new boundary pieces between already existing nodes would be meaningless, as we would have the same 3D plane on both sides. Therefore, we are left with four possible operations, which are illustrated in figure 4:

1. Unification of neighbored nodes by elimination of the boundary piece connecting them
2. Splitting of a node into two nodes by insertion of a new boundary piece connecting them.
3. Separation of a region into two pieces by tying it off in the middle.
4. Unification of two regions of the same 3D-plane which share a common node.

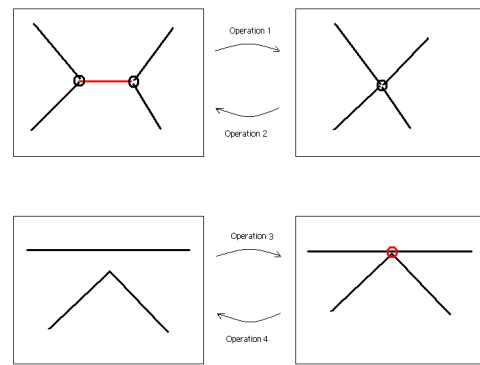


Figure 4: Topological Operations

Obviously operation 2 is the inverse to operation 1 and operation 4 is inverse to operation 3.

With the elimination or insertion of a boundary piece by operation 1 or operation 2, also an adjacency between two regions is eliminated or newly created, respectively. Operation 1 is only possible for nodes from which more than three boundary pieces are incident: If a node with three emanating boundary pieces is splitted, one of the resulting nodes features only two emanating boundary pieces and is therefore no node anymore, see figure 1(d). In fact, we shall lateron append edges to or cut away from existing boundary pieces, but these are not topological operations in the strict sense, as they let the adjacency relations between the regions unaltered.

Operations 3, 4 are exceptions from the requirement stated in the previous section, that new regions must not be inserted neither eliminated. By operation 3 possibly a new node is generated and possibly one or two boundary pieces are subdivided, by operation 4 possibly a node is eliminated and possibly one or two pairs of mutually adjacent boundary pieces are unified.

2–4 Proposed Algorithm

We propose the following algorithm:

1. Computation of approximate node coordinates
2. Elimination of “empty” boundary pieces by unification of the end nodes of the boundary piece (operation 1)
3. Combination of the edges of a boundary piece to a connected chain
4. Splitting of nodes according to the criteria given in subsection 2–6 (operation 2)
5. Consistency check for the loops according to the conditions 3a, b, c. If necessary, introduce new nodes (operation 3)
6. Global adjustment of the plane and edge parameters

After the global adjustment of the roof parameters, operations 2 and 4 could be applied additionally, if the residuals of certain elements are exceeding a preselected threshold.

2-5 Unification of Nodes

After the detection of edges by RANSAC, we shall probably be left with “empty” boundary pieces, i.e. boundary pieces to which no edges could be fitted. This may happen for the short sides of narrow regions between long parallel edges, but also if corners are “smeared” to very short boundary pieces by the plane fitting or the morphological filtering, respectively. We may wish to eliminate the latter kind of boundary pieces and retain the former. However, we prefer to eliminate in a first step *all* boundary pieces having no edges fitted to them, except if the “azimuth condition” 3a) of section 2-2 would be coarsely violated. Figure 5 shows an example, where the retaining of “empty” boundary pieces between parallels would lead to undesired results: In Fig-

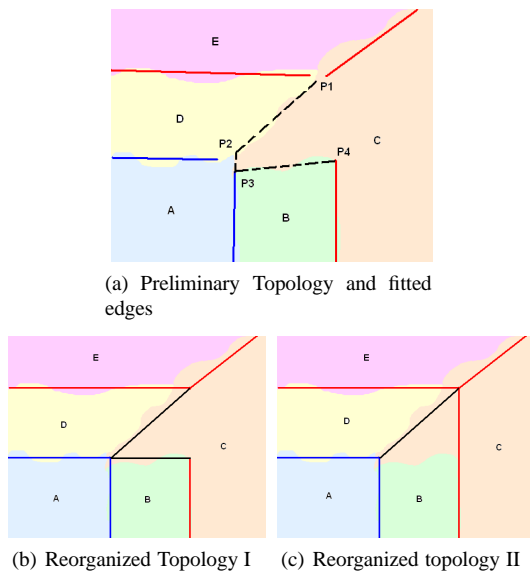


Figure 5: Reorganization of Topology; see text for explanation

ure 5(a) the situation after the line fitting is sketched. Regions C and E are weakly inclined roof surfaces, regions B and D feature the same horizontal direction of the normal vectors as C and E respectively, but are stronger inclined. For the boundary pieces ED, CE and BC I-edges have been accepted, for the boundary pieces AB and AD D-edges have been found. The boundary pieces AC, CD are empty. P3 and P4 so far represent the same node. Obviously figure 5(c) shows the “natural” topology for this situation, the more as the edges DE, BC and CE intersect nicely in point P1. However, if we retain the empty boundary piece CD with the argument that it forms the connection between the parallels AD, DE, we are not able to unify the points P1 and P4 and therefore we obtain the undesired solution illustrated in figure 5(b). If we eliminate all empty boundary pieces, we can easily generate the desired topology in the following step, the splitting of nodes, as will be shown.

Theoretically, there are cases for which the proposed proceeding fails, we did not encounter such a case in our numerical experiments, however.

2-6 Splitting of Nodes

We propose two criteria for the decision, if a node is to be split or not:

1. If two almost parallel edges are emanating nearly in the same direction from a node, the node is split into two nodes.

2. If the maximal distance between the intersection points of any neighbored edges emanating from the node exceeds a certain threshold, the node is split.
3. In both cases, all edges emanating from the old node have to be affiliated to one of the new nodes. If one of the new nodes is left with only one edge (apart from the new connection), the old node is not split, but a new edge is inserted between the node and the “solitary” edge.

For the last case, see figure 1(d) as an example.

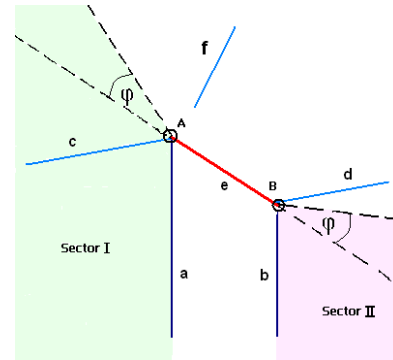


Figure 6: Splitting of Nodes I, for explanations see text

2-6.1 Case 1 Let us first consider the case of parallel edges. We try to determine approximate coordinates of the new nodes by intersecting each of the parallels with their non-parallel neighbours in the same node if existing, see figure 6 as an example: here the edges c, d can be used for intersection with the parallels a, b. If only one or no intersection point at all could be determined, we propose to insert a new edge between the parallels orthogonally, possibly using the mean of the original endpoints. Now the other edges emanating from the old node have to be associated with one of the two new nodes. Firstly we define:

Definition of directional sectors:

Let two directional sectors I, II in the horizontal plane be limited respectively by one of the parallel edges on the one side and the opposite direction of the newly inserted edge plus a chosen threshold angle φ on the other side.

As an example, see figure 6. We propose the following rules for the affiliation of edges to the new nodes:

1. Edges which meet the node in one of the two sectors I, II, are associated with the respective node.
2. Any edge which is situated outside the sectors I, II, is associated to that node, which features the smaller orthogonal distance to the respective edge.

According to the former rule, edge c in figure 6 is affiliated to node A, according to the latter rule, edge d is associated with node B. It is easy to see, that by these rules also the situation of figure 5 is resolved in the desired way.

2-6.2 Case 2 The case if the second criterion is fulfilled differs slightly from the case of parallel edges, see figure 7. Again, we intersect neighbored edges in order to compute approximate coordinates of the two new nodes. But here we use only intersections for which the mean node is situated *outside* of the smaller of the two sectors which are given by the intersecting edges. In figure 7 for instance the intersection point B' of the edges a, c

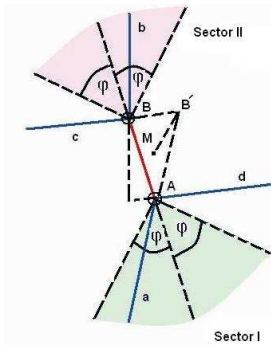


Figure 7: Splitting of Nodes II, for explanations see text

is excluded, because its connection B'M with the mean node M is situated within the directional sector spanned by the edges c, a. Proceeding in this way, we avoid non-admissible solutions as in figure 1(e). Now from all the non-excluded intersections in the node we select the two having their largest distance from the mean node as the new corner points and associate the edges of the node to one of the two intersections. We define

Definition of directional sectors:

Let two directional sectors I, II in the horizontal plane be limited respectively by the opposite direction of the newly inserted edge plus (for the one side) or minus (for the other side) a chosen threshold angle φ .

See figure 7 as an example. With these slightly different definitions of sectors compared to the case of parallel edges, we propose the same rules for the affiliation of edges as above:

1. Edges which meet the node in one of the two sectors I, II, are associated with the respective node.
2. Any edge which is situated outside the sectors I, II, is associated to that node, which features the smaller orthogonal distance to the respective edge.

A situation like in figure 1(a) can be resolved with the given rules.

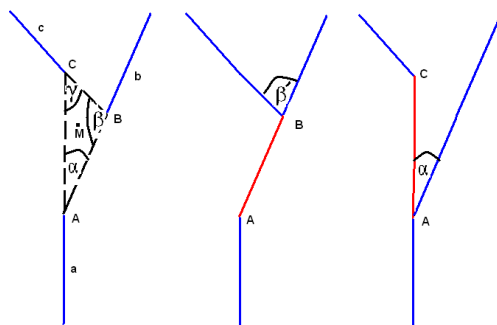


Figure 8: Splitting of Nodes III, for explanations see text

In either of the two cases we have proposed to affiliate edges according to their direction (within a certain directional sector) as the first criterion. Figure 8 shows that unlavely acute angles could appear if this criterion would be dropped. According to the "distance" criterion we would obtain the solution at the right, because the corners A, C have the biggest distance from the "mean node" M and edge b is closer (even incident) to A than to C. However,

the solution in the middle is preferable, as it avoids the acute angle α . This example also shows that it may be advisable to compute new approximate node coordinates after the affiliation of the edges.

3. ADJUSTMENT OF THE GEOMETRY

Once the topology has been reorganized, we are able to adjust the geometrical elements, i.e. the plane and edge parameters. Up to now the final horizontal position of the nodes has not yet been fixed, the edges emanating from a node do not exactly meet in a point in the horizontal plane. From a 3D point of view, the I-edges may be even warped. The necessary adjustment cannot be performed locally, i.e. for each node individually, because this would lead to non-planar roof surfaces. Therefore, we enforce the intersection of the edges in the nodes by means of a global adjustment. The "natural" model for the adjustment would be the conditioned adjustment with unknowns, where the plane and edge parameters enter as observations and the node coordinates represent the unknowns. In our experiments we were faced with ill-conditioned normal equations for this model, most probably due to linearly dependent conditions. Such a linear dependence e.g. occurs, if an I-edge is interrupted by crossing edges or regions, so that the edge is affiliated to more than two nodes. For this reason we prefer the common Gauss-Markov model with the conditions introduced as pseudo-observations. The plane and edge parameters as well as the approximate node coordinates are introduced as observations and as unknowns.

If a node features D-edges, it may have more than one height coordinate because the D-edges represent vertical walls in a 3D view. On the other hand, if two planar regions participating in a node are separated by an I-edge which is emanating from the node, they must have the same height coordinate in the node. We therefore classify the planar regions participating in a node into groups having the same height.

We use the plane equations in the following form:

$$x p_1 + y p_2 + z - p_3 = 0 \quad (3-2)$$

Here x, y denote the horizontal coordinates, z the height coordinate and p_1, p_2, p_3 the plane parameters. We prefer this formulation compared to the common implicit equation

$$x n_x + y n_y + z n_z - d = 0, \quad (3-3)$$

where n_x, n_y, n_z denote the components of the normal vector of the plane. As the normal vector features unit length, its components are not independent. Therefore, the covariance matrix with respect to the parameters n_x, n_y, n_z, d , which we obtain from the least squares fit within the RANSAC process, is singular! We can apply the former formulation, since we have excluded very steep planes so that in our case always $n_z > 0$. Obviously

$$p_1 = n_x/n_z, \quad p_2 = n_y/n_z, \quad p_3 = d/n_z \quad (3-4)$$

In the same way we have to avoid singular covariance matrices for the edge parameters and therefore use polar line parameters α, d :

$$x \cos \alpha + y \sin \alpha - d = 0 \quad (3-5)$$

Applying the plane and line equations (pseudo-observations), we obtain the following linearized observation equations for the planes and D-edges:

$$v - w = x_i dp_{k,1} + y_i dp_{k,2} - dp_{k,3} + p_{k,1} dx_i + p_{k,2} dy_i + dz_{i,j} \quad (3-6)$$

$$v - w = (y_i \cos \alpha_m - x_i \sin \alpha_m) d\alpha - dd_m + \cos \alpha_m dx_i + \sin \alpha_m dy_i \quad (3-7)$$

Here i represents the index of the respective node, k the index of the plane, j the index of the respective equivalence group within the node (of planes featuring the same height in the node). m represents the index of the respective edge. w represents the respective inconsistency and v the respective residual of the pseudo-observation. Edge-conditions are only introduced for D-edges as the parameters of the I-edges follow from the plane parameters. For the plane and D-edge parameters we introduce the covariance matrices which we have obtained from the RANSAC fit. For the condition pseudo-observations we introduce relatively strong, for the coordinate pseudo-observations relatively weak weights, of course.

As the plane parameters are much more reliable than the D-edge parameters, one may pose the question why the D-edges are introduced into the global adjustment at all. However, in a node where we have two parallel I-edges which are situated nearly parallel in opposite direction, the D-edges may be useful in order to stabilize the horizontal position of the node.

4. TEST COMPUTATIONS

As a test example for the proposed procedure we used the “Neue Schloss” of Stuttgart, a building which features various details. The company TopScan, Rheine, Germany kindly provided us LIDAR data covering the city of Stuttgart, Germany. The data have been interpolated on a regular grid with 0.5m grid size. By means of morphological segmentation we obtained the building area. Figure 9 shows a perspective contour plot of the Digi-

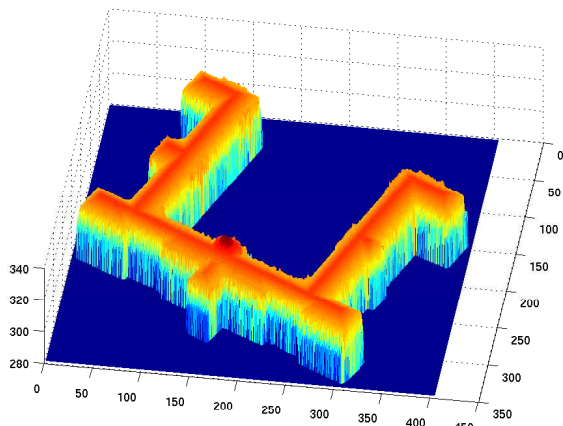


Figure 9: LIDAR DSM of Neues Schloss, Stuttgart

tal Surface Model of the Laser data. Figure 10 shows the segmented regions in the horizontal plane together with the adjusted edges. The topology is reorganized, the edges are completed. Each colour corresponds to a certain plane. I-edges appear in red, D-edges in black, edges of the building boundary in yellow. Due to the majority filtering, the situation looks quite homogeneous; small regions have been eliminated. Figure 11 finally represents a perspective view of the building model. In the central part of the building, a complicated steeple structure is located. Here RANSAC was not able to fit significant planes. Apart from this problematic zone, the model is satisfactory.

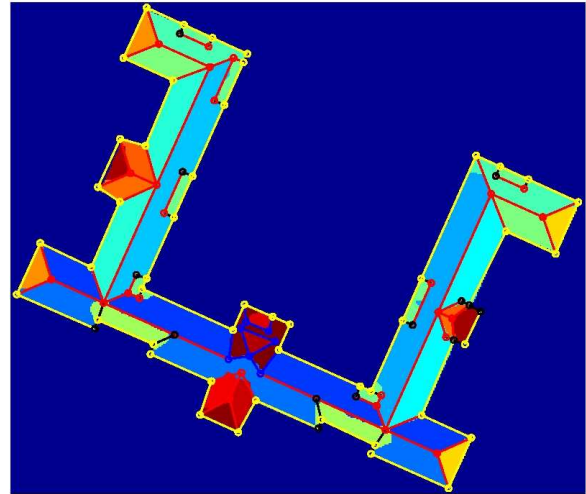


Figure 10: Topology reorganized, after adjustment

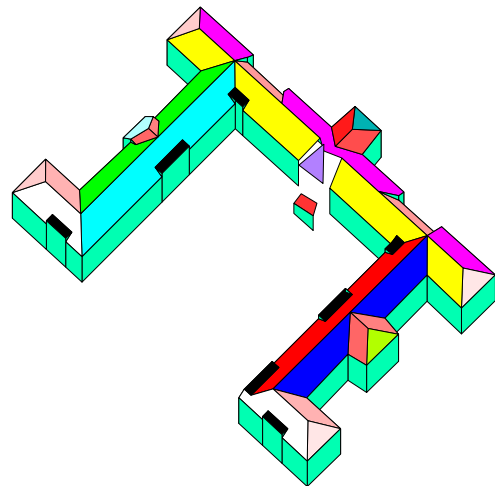


Figure 11: Topology reorganized, after adjustment, perspective view

5. CONCLUSIONS AND FUTURE WORK

Whereas the building reconstruction by means of volume primitives renders reliably complete building models, the generic approach presented here may leave undetermined regions and reacts sensitive to the preselected thresholds and parameters. On the other hand it turns out to be very flexible in the modelling of complicated building structures. Future work will concentrate on the improvement of the morphological filtering, the further development of topological operations and the reasonable filling of undetermined regions.

ACKNOWLEDGEMENTS

Funding for this research project (FoQus-on-AI) is provided by the German Federal Ministry of Education and Research. We also would like to thank three anonymous reviewers for their very helpful comments.

REFERENCES

- Alharty, A., and Bethel, J. 2004. Detailed building reconstruction from airborne laser data using a moving surface method. In: *Int. Archives of Photogrammetry and Remote Sensing*. Vol. XXXV - B3, pp. 213-218.
- Baltsavias, E., Grün, A., van Gool, L. (Eds.) 2001. Automatic Extraction of Man-Made Objects from Aerial and Space Images (III), Balkema Publishers.
- Haala, N. and Brenner, C. 1999. Extraction of Buildings and Trees in Urban Environments, *ISPRS Journal of Photogrammetry and Remote Sensing*, 54(2-3), pp. 130-137.
- Rottensteiner, F. 2003. Automatic generation of high-quality building models from Lidar data. *SilviLaser 2007' IEEE CG&A* 23(6), pp.42-51.
- Schenk, T. and Csatho, B. 2002. Fusion of Lidar Data and Aerial Imagery for a More Complete Surface Description. *Int. Archives of Photogrammetry and Remote Sensing*. Vol. XXXIV/3A, pp. 310-317.
- Séquin, C. Generalized Euler-Poincaré Theorem.
<http://www.cs.berkeley.edu/~sequin/PAPERS/EulerRel.pdf> (visited in April 2008).
- Tarsha-Kurdi, F., Landes, T. Grussenmeyer, P. 2007. Hough-Transform and Extended RANSAC Algorithms for Automatic Detection of 3D Building Roof Planes from Lidar Data. *Int. Archives of Photogrammetry and Remote Sensing*, Vol. XXXVI, PART 3/W52, pp. 407-412.
- Vosselman, G. and C. Brenner (Eds.) 2005. Proceedings of the ISPRS Workshop Laser Scanning 2005. *Int. Archives of Photogrammetry and Remote Sensing*. Vol. XXXVI, PART 3/W19.
- Vosselman, G. 1999. Building reconstruction using planar faces in very high density height data. In: *Int. Archives of Photogrammetry and Remote Sensing*, Vol. XXXII/3-2W5, pp. 87-92.